RSC Advances

This is an *Accepted Manuscript*, which has been through the Royal Society of Chemistry peer review process and has been accepted for publication.

Accepted Manuscripts are published online shortly after acceptance, before technical editing, formatting and proof reading. Using this free service, authors can make their results available to the community, in citable form, before we publish the edited article. This *Accepted Manuscript* will be replaced by the edited, formatted and paginated article as soon as this is available.

You can find more information about *Accepted Manuscripts* in the **Information for Authors**.

Please note that technical editing may introduce minor changes to the text and/or graphics, which may alter content. The journal's standard **Terms & Conditions** and the **Ethical guidelines** still apply. In no event shall the Royal Society of Chemistry be held responsible for any errors or omissions in this *Accepted Manuscript* or any consequences arising from the use of any information it contains.

Journal Name

ARTICLE

A rheological study on non-rubber component network in natural rubber

Lili Xu[a], Jing Zheng[b,*], Cheng Huang[b], Mingchao Luo[c], Wei Qu[c], Han Liu [c], Zhewei Gu[c], Liumei Jing[c] and Guangsu Huang[*]

Non-rubber components, mainly indicating phospholipid and protein, were separately removed from natural rubber to individually study their effect on structure and properties of the rubber. Fourier Transform Infrared Spectroscopy (FTIR) and ^{1}H nuclear magnetic resonance (^{1}H NMR) were applied to characterize the chemical structure and the non-rubber component residual. Rheology study and stress relaxation measurement were adopted to study the role non-rubbers played in natural networks. Rheological study of natural rubber (NR) and deproteinized natural rubber (DPNR) exhibited similar dynamic modulus at 170ºC. The lack of superposition in van Gurp Palmen (vGP) curves at different temperature for NR and DPNR, together with the shape of vGP curves proved that long chain branching was mainly constructed by phospholipid. Stress relaxation measurement at room temperature was fitted with Maxwell model and showed that NR relaxation curve underwent a quick decrease and then come to 58% equilibrium stress retention, about 3 times higher than that of DPNR, indicating that protein in NR contributed to the network structure at room temperature. Combined the chemical with molecule dynamic study, the interaction between protein and phospholipid in non-rubber component network was proposed.

Introduction

Natural rubber (NR) has been particularly interesting and attractive materials since their first vulcanization by C. Goodyear in 1839. And the natural rubber (NR) latex, collected from the *Hevea* trees as a colloidal suspension [1], is the main commercial feedstock for rubber and latex dipping industries. The field of tire industry is one for which the application of natural rubber is highly attractive, and obvious superiorities in mechanical and universal properties in a wide temperature range could allow such materials to be employed as innovative solutions to satisfy the demanding requirements that a modern-day tire must fulfill, such as wet grip, mechanical and thermal resistance, low cost, recycling, etc.[2, 3] Nowadays, natural rubber has become increasingly important for applications spanning many fields of chemistry, the hygienic and medical sectors, and it is further involved in a broad spectrum of consumer products in our daily life [4-7].

As a natural material, the yield of natural rubber which is restricted seriously by land resources and natural conditions, has become the fatal bottlenecks for extensive application. Under this circumstance, synthetic analogue polyisoprene with high expectations to replace natural rubber is modified mainly by various molecule design [8-13], while the comprehensive properties were disappointing.

It is reported that the non-rubbers [14], especially proteins and lipids, confer to the natural rubber latex excellent properties unsurpassed by any synthetic latex [15]. As a consequence, great industrial and scientific attention is paid to non-rubbers structure and their primary importance on natural rubber structure to construct the magical mechanical performance [16], such as high strength of raw rubber (green strength), shape retention, high tensile strength, high crack growth resistance and minimal heat built up in the vulcanized state. Several attempts have also been made to study the non-rubber components and investigate the corresponding structure in natural rubber. Tanaka, Y [17, 18] first proposed that cis-polyisoprenes obtained from H. brasiliensis and Parthenium aryentatum consist of more than 5000 isoprene units and that there are trans-isoprene units per rubber chain. And the mainstream view now is that the NR molecules comprise of 2 trans-isoprene units connected to a long-chain of cis-isoprene units. Two terminal groups, referred to as α and ω, have been postulated to link with mono- and di-phosphate groups associated with phospholipids by H-bonding at the α-terminal, whereas the ω-terminal is postulated to be a modified dimethylallyl group linked to protein by H-bonding [19]. Then the non-rubbers can connect the linear polyisoprene chains in NR through functional terminals and generate the branching or net-working topology, which intitules the "naturally occurring

network". [20]But since Goodyear medal [19] in 2001, no clear evidence of structure of end-linking network is reported yet.

Although the real cross-linking structure and role of non-rubbers are not fully understood, it was suggested that the cross-linking of NR formed by non-rubbers can be eliminated by deproteinization and transesterification. After the removal of protein and phospholipid, linear rubber chain can be obtained. [21]

The effect of proteins and phospholipids on strain induced crystallization and the correlation with the tensile strength of NR have been extensively studied by X-ray diffraction and microscopic methods [22, 23]. While spectroscopy method is static and mostly accompanied by solvent, and X-ray characterization is indirect in "natural occurring" networking characterization. Rheological property is highly sensitive to long chain branching because even a low degree of long-chain branching has a significant effect on the viscoelasticity in polyethylenes [23-28] or polypropylene [29]. Van Gurp Palmen curve, which was first proposed to judge the feasibility of Time-Temperature Superposition (TTS) principles and then evolved to branched structure study independent of chemical components of the macromolecule chain, is also very sensitive to the long chain branching of the polyisoprene melt in unvulcanized NR [30]. Therefore, the rheological behavior of unvulcanized NR can be characterized by a dynamic spectrum, related to molecular structure in melt, which is strongly impacted by branching or networking. However, to our knowledge, there is a lack of systematic investigation on how the non-rubber components, affect the rheological behavior of rubber chains in melt and inversively testify role of non-rubber components from rheology, especially effect of the long chain branching on rheological property. While few rheological studies were conducted in NR, among which most focused on blended NR with plastic [31], silica [32, 33], carbon black [34] or other natural ingredient [35] in vulcanized regime, and hardly any was on unvulcanized rubber. While in unvulcanized NR, the studies mainly emphasized on processability [36] or nonlinear viscoelastic behavior [37]. In this study, we conducted rheological study on the unvulcanized NR melt, and introduced the widely used vGP curve into unvulcanized NR to study the effect of non-rubber component.

Additionally, the stress relaxation behavior is also of important guiding sense in probing the network, additionally the equilibrium relaxation modulus G_∞ is proportional to crosslinking density. [28] The stress relaxation behavior of natural rubber is often investigated in vulcanized rubber [29-31], while scare reports in unvulcanized regime is reviewed if there were. In this study, to investigate the network structure constructed by non-rubbers in unvulcanized NR, we introduced stress relaxation test and analyze the equilibrium relaxation modulus to evaluate the crosslinking density and constraint to relaxation units.

In this work, an attempt was made to clarify the "naturally occuring network" by molecule dynamic study, combining the chemical structure analysis. Fourier Transform Infrared Spectroscopy (FTIR), Rheology and stress relaxation were applied to analyze the composition and structure of the natural network. To individually study the effect of non-rubber component, three models were prepared to individually study the effect of non-rubber component and listed as follows, NR containing all the non-rubber component, deproteined natural rubber (DPNR) containing phospholipid and fatty acid, transesterified deproteinized natural rubber (TEDPNR) containing only rubber chain.

Experimental

Materials

Natural rubber latex used in the present work was commercial high ammonia natural rubber (HANR) latex purchased from Dongfeng company (China). Total solid content and dry rubber content of the HANR latex, determined according to ASTM D 1076, were 61.3% and 60.8 w/w%, respectively. Triton X-100 and protease (P-5380) was provided from Sigma-Adrich. Other reagents used were analytical grade.

Preparation of specimens

Three models were prepared to individually study the effect of non-rubber component and listed as follows, natural rubber containing all the non-rubber component, deproteined natural rubber (DPNR) containing phospholipid and fatty acid, transesterified deproteinized natural rubber (TEDPNR) containing only rubber chain.

Natural rubber
HANR latex was centrifugation once for the removal of dash, and then spread into a thin layer to dry in under reduced pressure at ambient temperature until constant weight in vacuum oven.

Deproteinization of natural rubber
Deproteinization of the HANR latex was carried out by incubation with 0.08wt% protease in the presence of 0.15% v/v Triton X-100 and 1wt% aqua ammonia at 37℃ for 12h and the dry rubber content was 30%. The cream fraction was redispersed in the surfactant, in which dry rubber content was adjusted to 30wt% with deionized water. It was washed twice or three times by centrifugation. The rubber was recovered by centrifugation followed by coagulation with methanol and dried under reduced pressure at ambient temperature until constant weight.

Measurement of nitrogen content of the deproteined natural rubber (DPNR) was made by nitrogen elemental analyzer (CARLO ERBA 1106, Italian), and the nitrogen content was reduced from 0.5% to 0.07% after deproteinization.

Transesterification of the deproteined rubber
Transesterification of the rubber from DPNR was carried out in 2% w/v toluene by reaction with freshly prepared sodium methoxide and stirring at room temperature for 8h. The resulting transesterified deproteinized natural rubber (TEDPNR) was purified by precipitation of the rubber solution using excess of methanol and then dried in vacuum oven.

Measurement of phosphorus content of TEDPNR was made by phosphorus elemental analyzer (IRIS 1000 ICP-AES, Thermo Electron Co. USA), and the phosphorus content was reduced from 224ppm to 65ppm after transesterification.

The molecular weight of all samples was determined by gel permeation chromatography (HLC-8320, Waters), and the number averaged molecule weight was about 150-160kg mol^{-1} for NR and DPNR, 134kg mol^{-1} for TEDPNR, while MW of commercial linear isoprene rubber (IR) was 317 kg mol^{-1}.

Characterization

FTIR. The rubber samples for FTIR analysis were prepared by casting 1% w/v solutions of the rubber in tetrahydrofuran (THF) on a KBr disk, conducted with a Nicolet-560 infrared spectrometer (USA) using a potassium bromide (KBr) pellet. FTIR spectrums were recorded in the spectrumsl range of 4000-400 cm^{-1} with a 2 cm^{-1} resolution and 32 scans.

1H-NMR. 1H NMR spectra was recorded on a spectrometer (Varian INOVA-400) at 25°C using $CDCl_3$ as the solvent and TMS as the external standard.

Rheology Analysis. Dynamic mechanical measurements were performed by means of the HAAKE PXR800 rheometer. Shear deformation was applied under conditions of controlled deformation amplitude, always remaining in the range of linear viscoelastic response. Frequency dependencies of the storage (G') and loss (G") shear moduli were measured in the frequency range 0.01-100 Hz at a deformation amplitude ranging from 2 to 4% depending on temperature and at various temperatures between 160°C and 190°C. The geometry of parallel plates was employed with plate diameters of 20 mm and a sample thickness of 1.2 mm. Temperature control ((0.1°C) was achieved via water circulation system. Before measurements, the samples were processed into even thickness plate by heat-pressing at 150°C for 5 min in a mold and then isothermal for 12h in vacuum at 40°C.

Stress relaxation. Stress relaxation was conducted in INSTRONG universal tensile test machine at a proper strain of 20%. The total length was 15mm and elongated to target strain at 500mm min-1 tension rate and then keep the strain for 1200s. Before measurements, the samples were processed into even thickness plate by heat-pressing at 150°C for 5 min in a mold and then isothermal for 12h in vacuum at 40°C.

Results and discussion

Chemical structure characterization of NR samples

Infrared spectroscopy was used as a method of chemical structure analysis, and also to study intermolecular interactions caused by hydrogen bonding, because the vibrational modes of the donor and acceptor groups are sensitive to this interaction leading to a change in a vibrational characteristic [32]. And the FTIR spectrums of NR, DPNR and TEDPNR at room temperature were plotted in Fig.1.
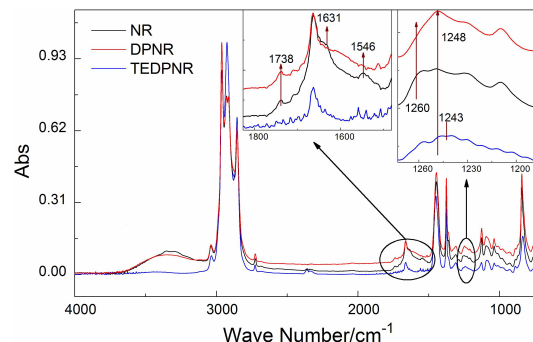

Fig.1 FTIR spectrum of the NR, DPNR and TEDPNR.

First, a wide H-bond peak at around 3400cm^{-1} was absent in TEDPNR. And in NR the wide peak comprised a relatively sharp peak at about 3300cm^{-1} related to the N-H symmetric stretch in H-bond, and the wide H-bond peak is mainly ascribed to O-H symmetric stretch in H-bond in non-rubbers, overlaping with small amount of environment water absorbed by non-rubbers.

Second, to pick out the non-rubbers, the rubber chain peaks assignment are listed below. vmax/cm[-1] 836 (Trisubstituted olefin out-of-plane =CH, wag), 1129 (-CH_3, rock), 1300 (-CH_2-, wag), 1376 (-CH_3, symmetric deformation), 1450 (-CH_2- symmetric and -CH_3 asymmetric deformation), 1664 (C=C, stretch), 2720 (Overtone of -CH_2- umbrella), 2850 (-CH_2- and -CH_3, symmetric stretch), 2920 (-CH_2-, asymmetric stretch), 2962 (-CH_3, asymmetric stretch), 3030 (Olefin =CH- stretch) [33, 34].

Then, the recession of characteristic peaks of protein at 1663 and 1546cm^{-1} [35] is obviously observed in DPNR compared with NR, and the peaks of C=O in phospholipid at 1738cm^{-1} [36] in TEDPNR. The FTIR results, combining with the elemental analysis in section 2, proved that the intended samples were successfully prepared. As for the different intensity of C=C strech peak in normalized infrared spectrogram, it can be interpreted by various infrared activity with different non-rubber environment.

The shoulder peak at 1260cm^{-1} in NR shifted to 1248cm^{-1} and turn sharp after protein removal, continually shifting to about 1243cm^{-1} and receding rapidly after phospholipid deprivation. It has been reported that the asymmetric O-P-O vibrational band is extremely sensitive to hydration, and the O-P-O asymmetric stretching of the hydrated phospholipid bilayer is usually observed at 1230 cm^{-1}, whereas dried or anhydrous lipid always appears at 30 cm^{-1} higher frequency. [37] The shift of O-P-O asymmetric stretching peak strongly suggests that phospholipids in NR interacted with protein via H-bond, and in DPNR rubber aggregate or link together via H-bond. [38]
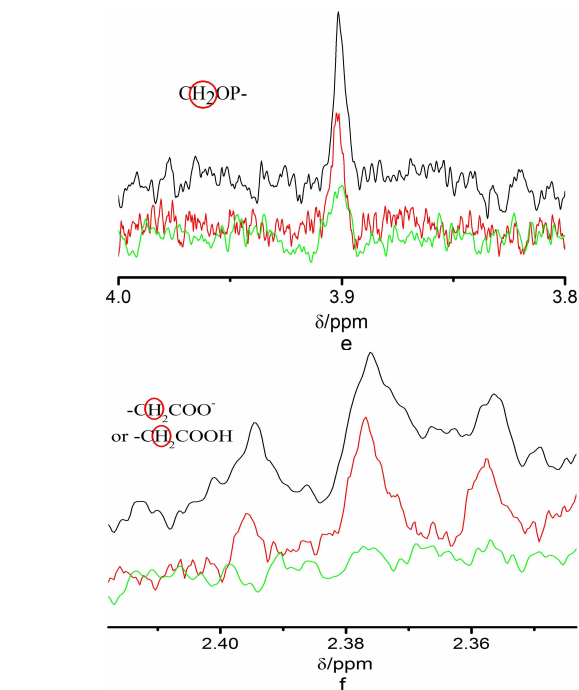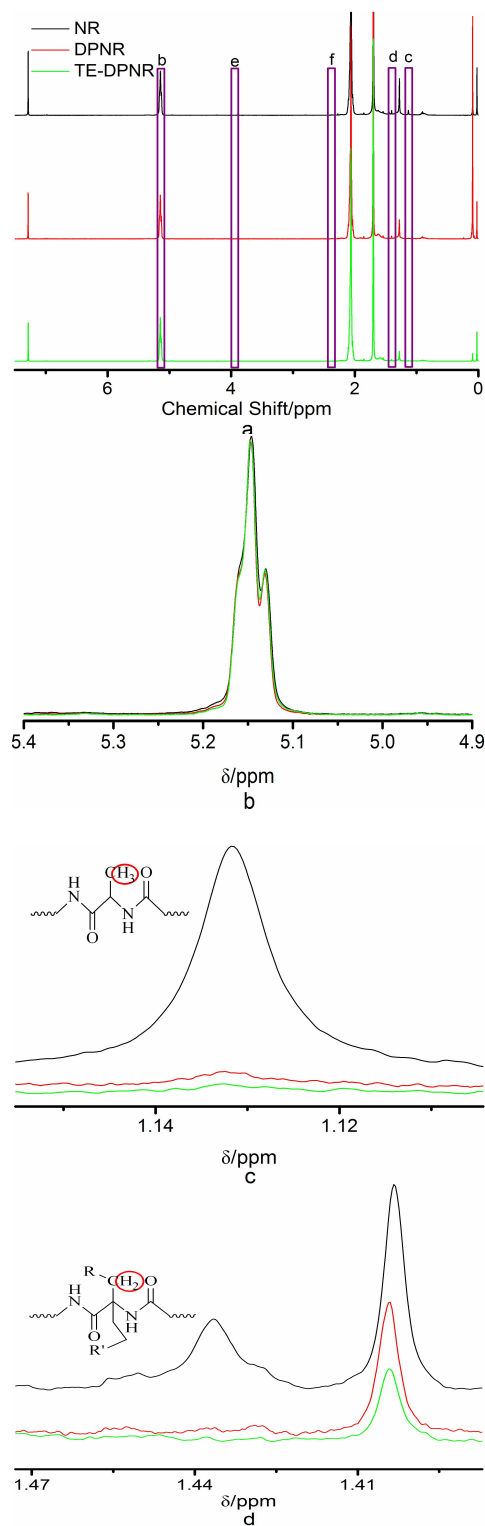
1H-NMR

Fig.2 (a) ^{1}H-NMR spectrums of NR, DPNR and TEDPNR in the range of 0-7.5ppm, extended ^{1}H-NMR spectrums of NR, DPNR and TEDPNR normalized by the peak of 5.15ppm in the range of (b)4.9-5.4ppm, (c) 1.10-1.16ppm, (d) 1.39-1.47ppm, (e) 3.80-4.00ppm, (f) 2.34-2.42ppm.

The ^{1}H-NMR spectrums of NR, DPNR and TEDPNR were shown in Fig.2, and a small amount of residual chloroform peak was detected at 7.28ppm. All the spectrums were normalized by the =C-H at the backbone triple (J=6.5Hz) peak at 5.15ppm. A small multiplet signals resonating at 3.91ppm was expected to be derived from the nonequivalent methylene protons linked to a phosphate group, -C$\underline{H}_2$OP-.[39] The mutiple paeks at 2.365ppm, 2.375ppm and 2.395ppm were assignable to -CH$_2$- of long-chain fat, the mutiple peak at 2.06ppm was assignable to -C$\underline{H}_2$- in the backbone, the single peak at 1.7ppmmwas assignable to -C$\underline{H}_3$ in the backbone), the mutiple paek at 1.43ppm was assigned to -C$\underline{H}_2$- of protein, the mutiple peak at 1.13ppm was assigned to -C$\underline{H}_3$ of protein. From the extended spectrums we can see that protein was removed after deproteinization, long-chain fat was eliminated after transesterification, while phospholipid was partly removed in TEDPNR. This can be interpreted that some phospholipid was connected with the rubber chain terminal. [16]

Combining ^{1}H-NMR and FTIR results, we can conclude that the intended samples were successfully prepared.

Branching molecular structure in unvulcanized nature rubber

To further study the effect of non-rubbers on the main chain structure, rheological behavior was analyzed in this section.

All measurements were conducted at a fixed strain, ranging from 2% to 4% at 170°C where all samples display the linear

viscoelastic performance respectively, and the storage modulus G′ as functions of frequency is shown in Fig. 3. At so high temperature, most H-bonding or other non-bonding interaction was destroyed at this temperature.
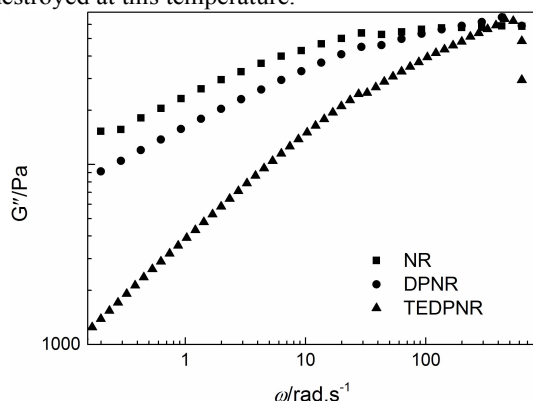

Fig.3 Dynamic spectrum of NR, DPNR and TEDPNR at 170ºC.

NR and DPNR show a higher modulus at low frequency than TEDPNR, indicating long-chain branching, crosslinking or phase-separation existence. [40, 41] However, the modulus of NR is a little higher than that of DPNR. DPNR displayed no apparent slope change at low frequency, while the modulus shifted up as much as 2 magnitudes contrasted with TEDPNR.
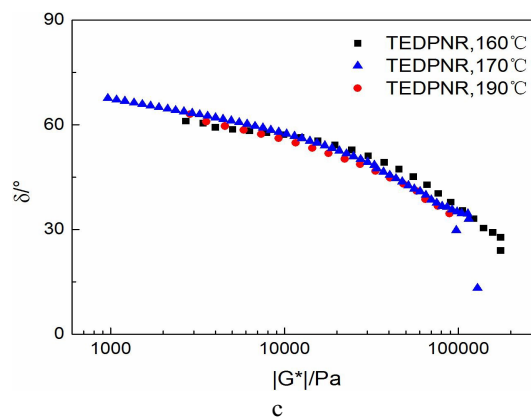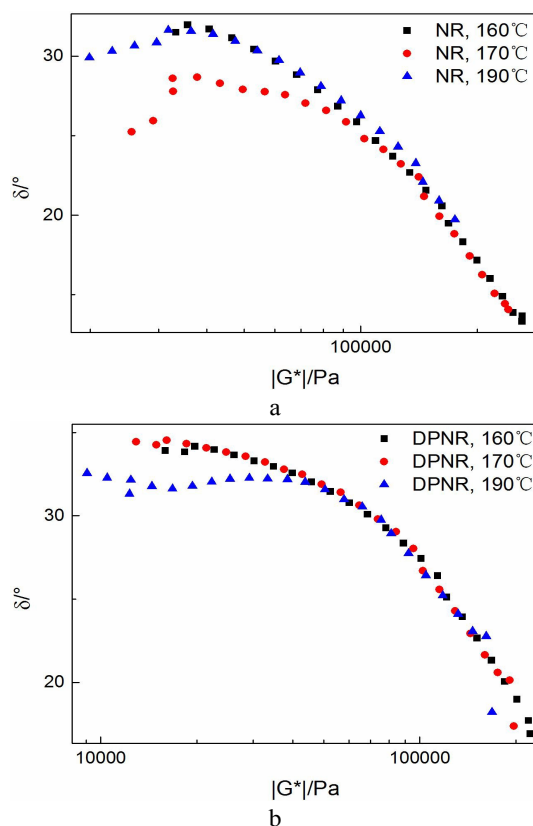

a

b

c

Fig.4 vGP curve of (a) NR, (b) DPNR and (c) TEDPNR at various temperatures.

To further investigate the modulus shift, dynamic spectrum in different temperatures for all samples were obtained, and van Gurp-Palmen plots were drawn from dynamic shear modulus at three different temperatures: 160, 170, and 190°C, displayed in Fig.3. Generally, fine superposition of vGP curves was observed for classical viscoelastic polymers, and little amount of long chain can significantly distort the vGP curve and thus cause a misalign. [42, 43] The rubber models were confirmed to be thermo-rheology melt from the discrepancy of vGP curves for NR and DPNR in Fig.4, possibly with long-chain branching or phase-separation.

To judge the reason of vGP curves discrepancy, temperature sweep from 100°C to 200°C in a frequency of 1 Hz at 1% strain was conducted. As is known, phase-separation can cause a sharp uprush in the modulus of temperature sweep. [44, 45] But now, the result shows no uprush in dynamic modulus in Fig.5, indicating that no phase separation occurred in the testing temperature region. As is shown in section 2, all samples were unvulcanized, so we can excluded the crosslinking. Now after excluding phase-separation, the modulus shift of NR and DPNR in Fig.3 is attributed to long chain branching, and a small amount of protein involved in forming long-chain branch.
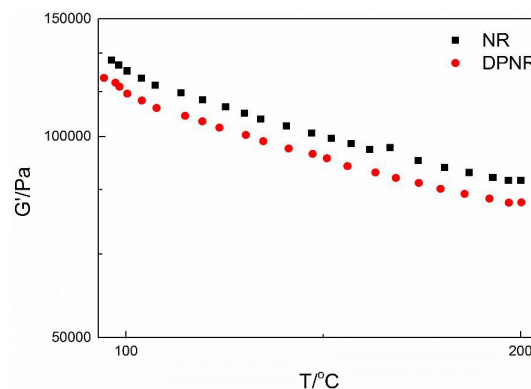

Fig.5 Temperature sweep in a frequency of 1 Hz at 1% strain from 100°C to 200°C.

In contrast to NR and DPNR, the overlap of vGP curves among the various temperature is good for TEDPNR, indicating that

TEDPNR is simple fluid. And from the shape of curve—only one minimum, spread monotonously to 90° in the phase angle—we can conclude that TEDPNR was probably linear. Combining the good linearity of Han map [46] in Fig.6, we can conclude that TEDPNR was linear at high temperature, in accordance with the dynamic spectrum.
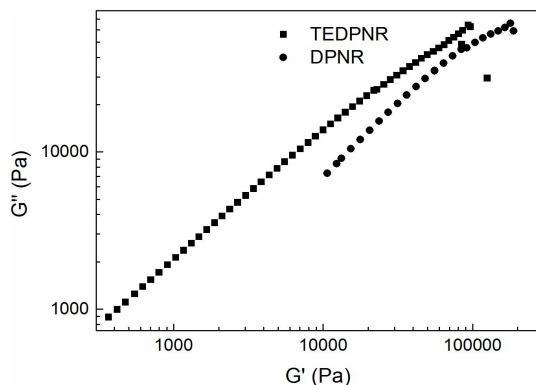

Fig.6 Han map of DPNR and TEDPNR at 170°C.

The above rheological results showed that long-chain branching existed only in NR and DPNR melt, indicating that phospholipid and a small amount of protein acted as the branching point in the long-chain branching construction. Furthermore, we can conclude, phospholipid and a small amount of protein connected with rubber terminal point by chemical bond or very strong interaction (survive at 170°C), then the non-rubbers coagulate by micellar interaction [47], and possibly formed star [48] in melt.

Netwok structure in unvulcanized nature rubber

Rheological demonstration on structure of three models at high temperature confirms the stable topology in NR, which proves in turn that the natural network is further constructed mainly by thermal unstable H-bonding or non-bond interaction between non-rubber component and rubber chain end, in accordance with the FTIR result. However, does the natural network exist in melt at room temperature? To answer this question, stress relaxation test was conducted. As is known, stress relaxation analysis is an effective method to study the network, and the equilibrium relaxation modulus G_∞ is proportional to crosslinking density. [44]

In this study, stress relaxation curves of NR, DPNR and TEDPNR at 25°C is displayed in Fig.7, where all samples were quickly subject to a proper strain of 20% to avoid the influence of strain induced crystallinity (SIC) [49], and then hold the strain for 1200s. For the sake of contrast, a relaxation curve of fairly linear IR with a 317kg mol^{-1} number average molecule weight (MW) was added. Generally, the stress of linear viscoelastic polymer quickly relaxed to a very small value, and even to zero.
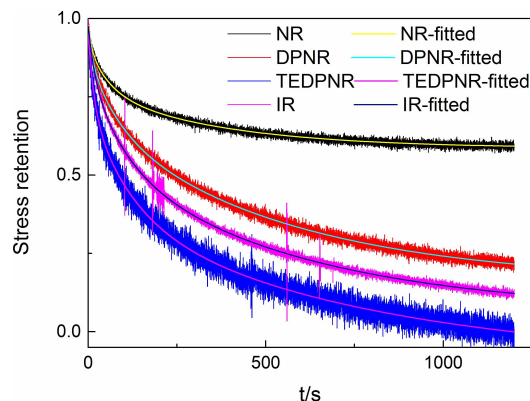

Fig.7 Stress relaxation curves of NR, DPNR, TEDPNR and IR at 25°C.

To illustrate the effect of non-rubbers on the stress relaxation tendency, all the instant stress was normalized by the corresponding initial stress, as is displayed in Fig.7. Relaxation curves of NR tended to form a plateau after about 300s and the retention is more than 50%, performed the largest stress retention, indicating that protein mainly contributed to the natural network at room temperature. Unexpectedly, DPNR performed nearly the same behaviors as that of IR, but relaxed slightly slower than that of linear IR. The TEDPNR relaxed to zero during the testing period. It can be confirmed that relaxation units in NR, were obviously confined by chemical or strong physical network. While in DPNR, the network constraint was scarcely observed in contrast to NR. However, comparing with linear IR, we can conclude that the restriction derived from long chain branching. TEDPNR displayed typical relaxation behavior of linear molecular chains with fully relaxed stress.

To further confirm the above assumption, we adopted Maxwell model [41, 50, 51] to describe the stress relaxation of rubber, read in equation 1:

$$\sigma(t) = \sigma_t + \sum \sigma_i e^{\frac{}{\tau_i}}$$

equ.1

In equation 1, $\sigma(t)$ represented the stress in the relaxation, σe was equilibrium stress, σi was coefficient of the ith Maxwell model and τi was relaxation time of the ith Maxwell model.

Elastomer relaxation followed a 7-element Maxwell model [52], read in equation 2:

$$\sigma(t) = \sigma_e + \sigma_1 e^{\frac{}{\tau_1}} + \sigma_2 e^{\frac{}{\tau_2}} + \sigma_3 e^{\frac{}{\tau_3}}$$

equ.2

Divided by the initial stress $\sigma 0$ in both sides, equation 2 may then be inverted to read:

$$\frac{\sigma(t)}{\sigma_0} = \frac{\sigma_e}{\sigma_0} + \frac{\sigma_1}{\sigma_0}e^{-\frac{t}{\tau_1}} + \frac{\sigma_2}{\sigma_0}e^{-\frac{t}{\tau_2}} + \frac{\sigma_3}{\sigma_0}e^{-\frac{t}{\tau_3}}$$

equ.3

Let $A(t) = \frac{\sigma(t)}{\sigma}$, $A0 = \frac{\sigma_e}{\sigma}$, $Ai = \frac{\sigma_i}{\sigma}$, $ti = \tau_i$

equ.4

Then we fit the experimental data by equation 3 and the result was listed in Table 1.

From equation 4, we can see that Ai represent the contribution of ti, and ti corresponds to the different relaxation unit in the samples. The A1, A2, A3 increased in the same samples with the increasing magnitude of the relaxation time t1, t2, t3. The consistency of Ai and ti proved that the larger relaxation unit contributed larger stress relaxation.

Table 1. The Maxwell fit result of stress relaxation at 25°C.

Sample	A0	A1	t1	A2	t2	A3	t3	R^2
NR	0.58507	0.06667	9.87772	0.13743	57.85191	0.18798	364.7487	0.9876
DPNR	0.15905	0.09697	12.62921	0.20228	82.65005	0.51581	544.9699	0.99534
IR	0.06292	0.13534	17.76458	0.27497	96.31696	0.50153	561.9759	0.99674
TEDPNR	-0.09715	0.21816	16.88401	0.33616	115.2694	0.48798	740.3617	0.9829

Second, the crosslinking density was discuss through the A0. As is shown in table 1, NR displays the largest A0, quadruple of DPNR, while A0 of DPNR is also higher than that in linear IR, and TEDPNR shows a meaningless negative A0.
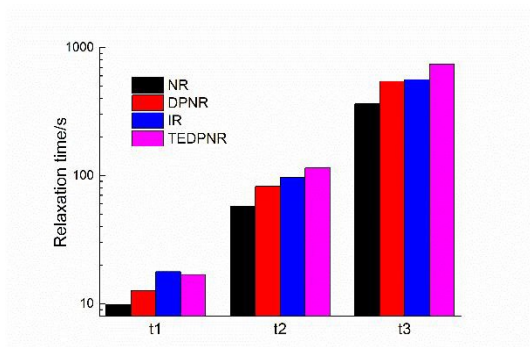

Fig.8 Maxwell relaxation time histogram of NR, DPNR, TEDPNR and IR.

From equation 4 we can see that A0 represented the stress retention rate, which is proportional to the equilibrium relaxation modulus $G\infty$ and crosslinking density, regardless of chemical or physical. Then we can conclude that NR possessed the largest cross-linking density, and the long chain branches in DPNR constructed small amount of strong entanglement network. From the 3 times higher crosslinking density, we can also conclude that part of the network structure in NR is connected by interaction between protein. Combined with the FTIR study, we can conclude that the interaction between protein and phospholipid can also contribute to the natural network, in accordance with the previous studies. [53, 54] For the linear IR, the super-high MW contributed to strong entanglement network, but was still weaker than in DPNR.

While in TEDPNR, the linear topology and lower MW results in the absence of strong entanglement network.

Then the relaxation time was also considered. And the relaxation time of all samples was displayed in the histogram in Fig.8.
As is shown in Fig.8, the relaxation time decrease in this order: NR<DPNR<IR<TEDPNR. In vulcanized rubber, the relaxation time decreases with increasing crosslinking density, which can be interpreted as the crosslinking point restriction. [38] Similarly, in the unvulcanized rubber, the relaxation units were also constrained by the natural network, and then displayed a decrease in relaxation time. The result confirmed that the crosslinking density increased in the order: NR>DPNR>IR>TEDPNR, which agreed with the previous study in A0.
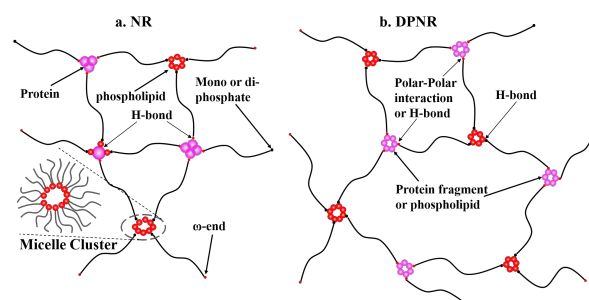
Scheme 1 Assumed network structure in (a) NR and (b) DPNR.

From the above results, we proposed the non-rubber in the structure of NR and DPNR in Scheme 1. In NR, the protein is connected in ω-terminal and then coagulated with each other by H-bond, part of which can also interact with phospholipid by H-bond. Moreover, in α-terminal, mono- or di-phosphate is bonded with the rubber chain, and then connected by micelle cluster. While in DPNR, the phospholipid or protein fragment after protease treatment can also interact with the ω-terminal by polar-polar interaction or H-bond, together with the α-terminal connected to phospholipid to form the network, whose density is much lower than that in NR.

Conclusions

The long chain branching point formed by phosphate, and crosslinking point consisted of protein and phospholipid are confirmed by the rheological and stress relaxation change of the three models. The modulus decreased at low frequcy, and equilibrium stress retention decreased by 75% after deproteinization, suggesting that the network was broken with removing protein. The van Gurp Palmen curves showed a fine overlap and the stress relaxed to zero after transesterification, indicating the decomposition of long chain branching point by phosphatase. The FTIR study of NR and DPNR further reveals that the H-bonding between protein and phosphatase connected with the terminal phosphatide mainly contributed to the physical crosslinking in NR. While in DPNR, part of phospholipid and protein fragments after protease treatment

may also connected with ω-terminal by H-bond to form the weak network, and H-bond between phosphatase and α-terminal phosphatide participated together in the formation of long chain branching point.

Notes and references

[a,b,c]College of Polymer Science and Engineering, State Key Laboratory of Polymer Materials Engineering, Sichuan University, Chengdu 610065, China.
email: Guangsu Huang@scu.edu.cn (G.S. Huang),
zhengjing@scu.edu.cn (J. Zheng)

1. Verhaar, G., Natural latex as a colloidal system. Rubber Chemistry and Technology, 1959. 32(5): p. 1627-1659.
2. Mitarai, K., Kneading carbon black and silica to a discharging temperature of 130 degrees c. or higher; nonhardening on storage, 2004, Google Patents.
3. Li, X., et al., Experimental study on the temperature dependence of hyperelastic behavior of tire rubbers under moderate finite deformation. Rubber Chemistry and Technology, 2011. 84(2): p. 215-228.
4. Bitinis, N., et al., Structure and properties of polylactide/natural rubber blends. Materials Chemistry and Physics, 2011. 129(3): p. 823-831.
5. Wrangsjö, K., et al., Primary prevention of latex allergy in healthcare—spectrum of strategies including the European glove standardization. Contact dermatitis, 2012. 66(4): p. 165-171.
6. Quitmann, D., et al., Solvent-sensitive reversible stress-response of shape memory natural rubber. ACS Appl Mater Interfaces, 2013. 5(9): p. 3504-7.
7. Elango, N. and A. Faudzi, A review article: investigations on soft materials for soft robot manipulations. The International Journal of Advanced Manufacturing Technology, 2015: p. 1-11.
8. Jitchum, V. and S. Perrier, Living radical polymerization of isoprene via the RAFT process. Macromolecules, 2007. 40(5): p. 1408-1412.
9. Schoenberg, E., et al., Polyisoprene. Rubber Chemistry and Technology, 1979. 52(3): p. 526-604.
10. Schoenberg, E., D. Chalfant, and R. Mayor, Preformed Aluminum Triisobutyl-Titanium Tetrachloride Catalysts for Isoprene Polymerization. Rubber chemistry and technology, 1964. 37(1): p. 103-120.
11. Kaita, S., et al., An efficient gadolinium metallocene-based catalyst for the synthesis of isoprene rubber with perfect 1, 4-cis microstructure and marked reactivity difference between lanthanide metallocenes toward dienes as probed by butadiene-isoprene copolymerization catalysis. Macromolecules, 2004. 37(16): p. 5860-5862.
12. Yuan, Z. and M. Gauthier, Synthesis of arborescent isoprene homopolymers. Macromolecules, 2005. 38(10): p. 4124-4132.
13. Uhrig, D. and J.W. Mays, Synthesis of combs, centipedes, and barbwires: poly (isoprene-graft-styrene) regular multigraft

14. Tarachiwin, L., Y. Tanaka, and J. Sakdapipanich, Structure and origin of long-chain branching and gel in natural rubber. Kautschuk Gummi Kunststoffe, 2005. 58(3): p. 115-122.
15. Hasma, H. and A. Subramaniam, Composition of lipids in latex of Hevea brasiliensis clone RRIM 501. J Nat Rubber Res, 1986. 1: p. 30-40.
16. Tanaka, Y. Structural characterization of naturally occurring cis-and trans-polyisoprenes by 13C-NMR spectroscopy. in J. Appl. Polym. Sci., Appl. Polym. Symp. 1989.
17. Tanaka, Y., et al., Initiation of biosynthesis in cis polyisoprenes. Phytochemistry, 1995. 39(4): p. 779-784.
18. Tarachiwin, L., et al., Structural characterization of α-terminal group of natural rubber. 2. Decomposition of branch-points by phospholipase and chemical treatments. Biomacromolecules, 2005. 6(4): p. 1858-1863.
19. Tanaka, Y., Structural characterization of natural polyisoprenes: solve the mystery of natural rubber based on structural study. Rubber chemistry and technology, 2001. 74(3): p. 355-375.
20. Toki, S., et al., Multi-scaled microstructures in natural rubber characterized by synchrotron X-ray scattering and optical microscopy. Journal of Polymer Science Part B: Polymer Physics, 2008. 46(22): p. 2456-2464.
21. Tangpakdee, J. and Y. Tanaka, Characterization of sol and gel in Hevea natural rubber. Rubber chemistry and technology, 1997. 70(5): p. 707-713.
22. Carretero-Gonzalez, J., et al., Real-time crystallization of organoclay nanoparticle filled natural rubber under stretching. Macromolecules, 2008. 41(7): p. 2295-2298.
23. Vega, J., et al., Small-amplitude oscillatory shear flow measurements as a tool to detect very low amounts of long chain branching in polyethylenes. Macromolecules, 1998. 31(11): p. 3639-3647.
24. Shen, H.W., et al., Rheological behaviors and molecular weight distribution characteristics of bimodal high‐density polyethylene. Journal of Applied Polymer Science, 2011. 121(3): p. 1543-1549.
25. Wood-Adams, P.M. and J.M. Dealy, Using rheological data to determine the branching level in metallocene polyethylenes. Macromolecules, 2000. 33(20): p. 7481-7488.
26. Hugo Rolón-Garrido, V.c., M. Zatloukal, and M.H. Wagner, Increase of long-chain branching by thermo-oxidative treatment of LDPE: Chromatographic, spectroscopic, and rheological evidence. Journal of Rheology, 2013. 57(1): p. 105.
27. Rolón‐Garrido, V.H., J. Luo, and M.H. Wagner. Increase of Long‐chain Branching by Thermo‐oxidative Treatment of LDPE. in NOVEL TRENDS IN RHEOLOGY IV. 2011. AIP Publishing.
28. Iedema, P.D., et al., Development of MWD and branching during peroxide modification of High-Density Polyethylene by SEC-MALS and Monte Carlo simulation. Polymer, 2013. 54(16): p. 4093-4104.
29. Zulli, F., et al., Rheology of long‐chain branched polypropylene copolymers. Journal of Applied Polymer Science, 2013. 127(2): p. 1423-1432.
30. Trinkle, S., P. Walter, and C. Friedrich, Van Gurp-Palmen plot II– classification of long chain branched polymers by their topology. Rheologica Acta, 2002. 41(1-2): p. 103-113.

31. Nakason, C., Y. Panklieng, and A. Kaesaman, Rheological and thermal properties of thermoplastic natural rubbers based on poly (methyl methacrylate)/epoxidized‐natural‐rubber blends. Journal of applied polymer science, 2004. 92(6): p. 3561-3572.

32. Zhang, F., et al., Network evolutions in both pure and silica-filled natural rubbers during cyclic shear loading. RSC Advances, 2014. 4(51): p. 26706.

33. Meera, A., et al., Nonlinear viscoelastic behavior of silica-filled natural rubber nanocomposites. The Journal of Physical Chemistry C, 2009. 113(42): p. 17997-18002.

34. Leblanc, J.L., Large amplitude oscillatory shear experiments to investigate the nonlinear viscoelastic properties of highly loaded carbon black rubber compounds without curatives. Journal of Applied Polymer Science, 2008. 109(2): p. 1271-1293.

35. Byars, J.A. and L. Jong, Flow properties of natural rubber composites filled with defatted soy flour. Journal of Applied Polymer Science, 2009. 111(4): p. 2049-2055.

36. Kim, C., et al., Better characterization of raw natural rubber by decreasing the rotor speed of Mooney viscometer: Role of macromolecular structure. Polymer Engineering & Science, 2010. 50(2): p. 240-248.

37. Leblanc, J.L., Nonlinear viscoelasticity of (unvulcanized) natural rubber, derived materials, and compounds through LAOS testing. Rubber Chemistry and Technology, 2010. 83(1): p. 65-96.

38. Batra, A., C. Cohen, and L. Archer, Stress relaxation of end-linked polydimethylsiloxane elastomers with long pendent chains. Macromolecules, 2005. 38(16): p. 7174-7180.

39. Tarachiwin, L., et al., Structural characterization of alpha-terminal group of natural rubber. 1. Decomposition of branch-points by lipase and phosphatase treatments. Biomacromolecules, 2005. 6(4): p. 1851-1857.

40. Berry, J. and W. Watson, Stress relaxation of peroxide and sulfur vulcanizates of natural rubber. Journal of Polymer Science, 1955. 18(88): p. 201-213.

41. Baeurle, S.A., A. Hotta, and A.A. Gusev, A new semi-phenomenological approach to predict the stress relaxation behavior of thermoplastic elastomers. Polymer, 2005. 46(12): p. 4344-4354.

42. Tobolsky, A.V., I.B. Prettyman, and J.H. Dillon, Stress Relaxation of Natural and Synthetic Rubber Stocks. Journal of Applied Physics, 1944. 15(4): p. 380.

43. Tobolsky, A.V., Stress Relaxation Studies of the Viscoelastic Properties of Polymers. Journal of Applied Physics, 1956. 27(7): p. 673.

44. Winter, H.H., Analysis of Linear Viscoelasticity of a Crosslinking Polymer at the Gel Point. Journal of Rheology, 1986. 30(2): p. 367.

45. Onogi, S., T. Matsumoto, and Y. Warashina, Rheological properties of dispersions of spherical particles in polymer solutions. Transactions of The Society of Rheology (1957-1977), 1973. 17(1): p. 175-190.

46. Hatzikiriakos, S.G., Long chain branching and polydispersity effects on the rheological properties of polyethylenes. Polymer Engineering & Science, 2000. 40(11): p. 2279-2287.

47. Yunyongwattanakorn, J., et al., Effect of gel on crystallization behavior of natural rubber after accelerated storage hardening test. Journal of Applied Polymer Science, 2007. 106(1): p. 455-461.

48. He, C., et al., Molecular structure of high melt strength polypropylene and its application to polymer design. Polymer, 2003. 44(23): p. 7181-7188.

49. Murakami, S., et al., Structural development of natural rubber during uniaxial stretching by in situ wide angle X-ray diffraction using a synchrotron radiation. Polymer, 2002. 43(7): p. 2117-2120.

50. Bernstein, B., E. Kearsley, and L. Zapas, A study of stress relaxation with finite strain. Transactions of The Society of Rheology (1957-1977), 1963. 7(1): p. 391-410.

51. Stevenson, J.S. and R.P. Kusy, Force application and decay characteristics of untreated and treated polyurethane elastomeric chains. The Angle Orthodontist, 1994. 64(6): p. 455-466.

52. Johnson, A. and C. Quigley, A viscohyperelastic Maxwell model for rubber viscoelasticity. Rubber chemistry and technology, 1992. 65(1): p. 137-153.

53. Nussinovitch, A., et al., Characterization of gellan gels by uniaxial compression, stress relaxation and creep 1. Journal of Texture Studies, 1990. 21(1): p. 37-50.

54. Tang, J., M.A. Tung, and Y. Zeng, Characterization of gellan gels using stress relaxation. Journal of food engineering, 1998. 38(3): p. 279-295.

55. Berthelot, K., et al., Rubber elongation factor (REF), a major allergen component in Hevea brasiliensis latex has amyloid properties. 2012.

56. Berthelot, K., et al., Rubber particle proteins, HbREF and HbSRPP, show different interactions with model membranes. Biochim Biophys Acta, 2014. 1838(1 Pt B): p. 287-99.

Protein can also interact with phospholipid, while in DPNR, phospholipid or protein fragment after can also interact with the ω-terminal.